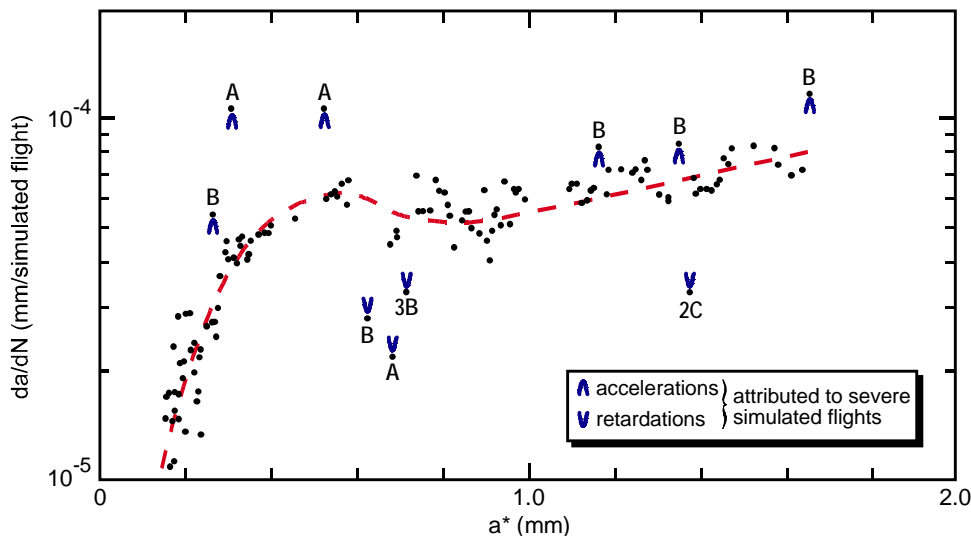




Executive summary

Fractography-based estimation of fatigue crack "initiation" and growth lives in aircraft components



Fractographically determined fatigue crack growth rates for a 7175-T73 forged aluminium window frame from a full-scale pressure cabin test under flight simulation loading

Problem area

Guidelines and procedures are given for fractography-based methods of estimating fatigue crack "initiation" and growth lives in aerospace materials and components.

Description

This report relies mainly on the knowledge from more than 30 years of fractographic analysis of fatigue fracture surfaces at the NLR. The topics are: preliminary procedures; crack "initiation"; constant amplitude crack growth; constant amplitude + marker loading crack growth; flight simulation loading crack growth with markers; and spectrum fatigue crack growth *per se*.

Examples are given for MSD (Multiple Site Damage) in pressure cabins; vertical stabilizer cracks from a full-scale test; low-cycle fatigue of a simulated fir-tree root in a turbine disc; cracks in a window panel from a barrel test; and in-service failure of an air supply manifold support rod from a military jet engine.

Applicability

The guidelines, procedures and examples in this report demonstrate the NLR's capabilities for fractographic analysis of fatigue failures, and may also be useful for other test and service failure investigators.

Report no.

NLR-TP-2006-184

Author(s)

R.J.H. Wanhill
T. Hattenberg

Classification report

Unclassified

Date

December 2006

Knowledge area(s)

Vliegtuigmateriaal- en schadeonderzoek

Descriptor(s)

fatigue
crack growth
fractography

This report is based on a presentation held at SIF 2006, Sydney, September 2006.

Fractography-based estimation of fatigue crack "initiation" and growth lives in aircraft components

Nationaal Lucht- en Ruimtevaartlaboratorium, National Aerospace Laboratory NLR

Anthony Fokkerweg 2, 1059 CM Amsterdam,
P.O. Box 90502, 1006 BM Amsterdam, The Netherlands
Telephone +31 20 511 31 13, Fax +31 20 511 32 10, Web site: www.nlr.nl



NLR-TP-2006-184

Fractography-based estimation of fatigue crack "initiation" and growth lives in aircraft components

R.J.H. Wanhill and T. Hattenberg

This report is based on a presentation held at SIF 2006, Sydney, September 2006.

The contents of this report may be cited on condition that full credit is given to NLR and the authors.

This publication has been refereed by the Advisory Committee AEROSPACE VEHICLES.

Customer National Aerospace Laboratory NLR
Contract number ----
Owner National Aerospace Laboratory NLR
Division Aerospace Vehicles
Distribution Unlimited
Classification of title Unclassified
September 2007

Approved by:

Author	Reviewer	Managing department

Summary

Guidelines and procedures are given for fractography-based methods of estimating fatigue crack “initiation” and growth lives in aerospace materials and components. The guidelines and procedures represent mainly the experience from more than 30 years of fractographic analysis of fatigue fracture surfaces at the NLR. The topics are:

- preliminary procedures
- crack “initiation”
- crack growth under constant amplitude loading
- crack growth under constant amplitude + marker loading
- crack growth under flight simulation loading with intentional marker features
- spectrum fatigue crack growth *per se*.

Examples illustrating these topics are given for MSD (Multiple Site fatigue Damage) in conventional aluminium alloy pressure cabins, both from service and full-scale tests; cracks in a vertical stabilizer rib and main hinge fitting from a Fokker 100 full-scale test; elevated temperature low-cycle fatigue of a nickel-base superalloy specimen simulating a fir tree root in a gas turbine disc; cracking in GLARE (GLASS REinforced aluminium laminate) panels and aluminium alloy window frames from the Airbus MegaLiner Barrel test; and failure of an air supply manifold support rod from a military jet engine.

Contents

1	Introduction	7
2	Preliminary procedures	8
3	Fatigue crack “initiation”	9
4	Constant amplitude crack growth fractography	10
4.1	Example of striation-based modelling	11
4.2	Example of striation-based analysis unsuited to modelling	12
5	Constant amplitude plus markers fractography	13
5.1	Marker band analysis	13
5.2	Marker band + striation analysis	14
6	Flight simulation plus markers fractography	15
7	Spectrum fatigue analysis	16
7.1	Airbus MLB window area fractography	16
7.2	Air supply manifold support rod failure	18
8	Concluding remarks	20
	References	21

3 Tables

21 Figures

(40 pages in total)

1 Introduction

This paper provides guidelines that apply to fractography-based methods of estimating fatigue crack “initiation” and growth lives. The guidelines are based on more than 30 years of accumulated expertise at the NLR.

These fractography-based methods rely on measurements of the spacings and positions of so-called *fatigue striations* and/or intermittent crack front *marker bands* on fatigue fracture surfaces.

Materials for which fatigue striations are readily visible include aerospace aluminium alloys, austenitic stainless steels and nickel-base superalloys. Striations are also visible on the fatigue fracture surfaces of high strength steels and titanium alloys, but can be ill-defined or replaced largely by other fatigue fracture mechanisms, particularly at low growth rates.

Even for materials that usually show well-defined fatigue striations there are a number of caveats. These are specified here with the aid of figure 1:

- Striation spacings do not necessarily correspond to the macroscopic crack growth rates, even approximately. At high growth rates the striation spacings underestimate the macroscopic rates because microvoid coalescence also contributes to cyclic crack growth. And at low crack growth rates there appears to be a lower limit to striation spacings. Lynch (2006)^[1] quotes this limit as generally being about 100nm, but we have often seen striations of 20 – 25nm spacing on fatigue fracture surfaces of the widely used AlCuMg alloy 2024–T3. Be that as it may, caution is sometimes required, as discussed in detail by Nedbal *et al.* (1984, 1989)^[2,3].
- The qualification “air environment” in figure 1 is advisable but not essential. Striations are best visible from fatigue in mild environments like normal air. More aggressive environments such as salt water or high temperature air can damage and eventually obscure the original fracture surface by corrosion and oxidation.
- The qualification “constant amplitude loading” in figure 1 is also important. When fatigue crack growth occurs under variable amplitude loading it may be difficult or impossible to make estimates of macroscopic crack growth rates from striation spacings. Much will depend on the type and complexity of the variable amplitude load history. This is discussed further in sections 5 – 7 of this paper.

2 Preliminary procedures

Table 1 lists the preliminary procedures that should be carried out before detailed fractography. Note that optical fractography is included. It is most important that this is done thoroughly.

Table 1 Preliminary procedures

<p><u>Sample documentation</u></p> <ul style="list-style-type: none">- location, geometry- material(s), surface treatments- cycles and/or (simulated) flights, flight hours- type of fatigue loading- load spectra and load histories (if known) <p><u>NDI of unopened cracks and suspect areas</u></p> <ul style="list-style-type: none">- visual- eddy current, ultrasound, penetrant, X-ray- record and number cracks and their locations <p><u>Forcible opening of cracks</u></p> <ul style="list-style-type: none">- e.g. see figure 2: note <i>precision</i> sawcuts <p><u>Macrofractography</u></p> <ul style="list-style-type: none">- visual , stereobinocular + diffuse lighting- crack initiation positions, possible causes- crack front shapes and sizes; marker bands- B&W and/or colour fractographs, $\leq 30\times$- optical fractograph photomontages
--

3 Fatigue crack “initiation”

Table 2 lists the observational aspects that may be involved in the detailed fractography of fatigue crack “initiation”. The use of quotation marks, “ ”, has the following reason.

Over the last four decades there has been much discussion about the existence of fatigue crack initiation. Some researchers and regulatory authorities contend or assume that crack growth begins during the very first load cycle, and so the concept of a fatigue initiation life is illusory or can be ignored.

On the other hand, there is irrefutable evidence that fatigue crack initiation in metals is a physical reality that is preceded by cumulative microstructural changes owing to the fatigue cycles, e.g. Plumbridge and Ryder (1969)^[4], Mughrabi (1980)^[5] and Jameel *et al.* (2003)^[6].

A generally acceptable definition of fatigue crack initiation life does not seem to be possible. However, a reasonable engineering definition is to take “initiation” to be the fatigue life beyond which there is a regular process of crack growth (Wanhill *et al.* 2001)^[7].

Table 2 Fractography of fatigue crack “initiation”

<p><u>Crack “initiation” positions</u></p> <p><u>Single or multiple initiation sites</u></p> <ul style="list-style-type: none"> - initiation “lengths” or “widths” for contiguous sites <p><u>Specific causes</u></p> <ul style="list-style-type: none"> - fretting, corrosion pits - material discontinuities, fabrication defects <p><u>Obscuration</u></p> <ul style="list-style-type: none"> - fretting products (oxide debris) - corrosion, e.g. “mud cracking”, “cauliflowers” - high temperature oxidation

Another important aspect included in table 2 is the question of material discontinuities or defects. Many engineering alloys *normally* contain discontinuities such as intermetallic inclusions, dispersoids, and even small voids: titanium alloys are (or should be) notable exceptions. The discontinuities are tolerated within specified limits, which depend on the material type and quality. Fatigue cracks can start to grow from the discontinuities, but if these are within the specifications it is inappropriate to refer to them as “defects”.

4 Constant amplitude crack growth fractography

This category includes fatigue tests under constant amplitude loading and fatigue tests and service fatigue cracking under *effectively* constant amplitude loading. Examples of the latter are vibratory fatigue of a helicopter rotor blade (Wanhill *et al.* 1974)^[8], cracking in a vertical stabilizer rib (Hattenberg and Vlieger 1993)^[9], and Multiple Site fatigue Damage (MSD) in pressure cabin lap splices (Wanhill *et al.* 2001)^[7].

Table 3 lists observational aspects that are, or may be, involved in the detailed fractography of constant amplitude fatigue fracture surfaces, including the measurement of striation spacings, which is the main topic in this section. A special mention should be made about oxidation interference colours. These can be helpful in estimating fatigue crack growth periods (Wanhill 2004)^[10], as discussed further in subsection 7.2.

Table 3 Detailed constant amplitude fractography

<p><u>Crack fronts</u></p> <ul style="list-style-type: none"> - coalescence of multiple cracks - crack front shapes and sizes <p><u>Overall topography</u></p> <ul style="list-style-type: none"> - faceted, semi-faceted - continuum-mode, i.e. including striations <p><u>Striations</u></p> <ul style="list-style-type: none"> - orientations, helping to estimate intermediate crack front developments - spacings in selected directions <p><u>Environmental effects</u></p> <ul style="list-style-type: none"> - progression (“beach”) marks - obscuration by corrosion, e.g. “mud cracking”, “cauliflowers” - high temperature oxidation and interference colours

A conventional Scanning Electron Microscope (SEM) may be sufficient for detailed fractography of some fatigue fracture surfaces. However, the superior resolution of a Field Emission Gun Scanning Electron Microscope (FEG-SEM) can be essential (Wanhill *et al.* 2001)^[7]. A FEG-SEM’s resolution approaches that obtainable from Transmission Electron Microscopy (TEM) of fracture surface replicas, and is certainly much easier to use. With care, a FEG-SEM can resolve fatigue striations down to 20 – 25nm for some materials, as mentioned in section 1.

Figure 3 illustrates the measurement of striation spacings in selected directions for an MSD crack in a pressure cabin longitudinal lap splice. This example has been chosen to demonstrate striation-based empirical modelling of fatigue crack growth, to be discussed in subsection 4.1. But first we note that despite the scatter in striation spacings, the average data in the lower graphic in figure 3 are represented by an equation of the form $da/dN = Ae^{Ba}$, where in this particular case $A = 0.06386$ and $B = 0.1938$. Assuming that the life, N_f , at the final crack length, a_f , is known, this type of equation is easily used to obtain estimates of (a) crack "initiation" lives, N_i , for any specified initial crack size, e.g. a_i in figure 3, and (b) crack growth lives, $N_f - N_i$, from

$$N_f - N_i = \frac{1}{AB} \left(e^{-Ba_i} - e^{-Ba_f} \right) \quad (1)$$

As discussed in subsection 5.2, equations of the form $da/dN = Ae^{Ba}$ also applied to striation spacings *versus* crack length for high temperature fatigue crack growth in nickel-base superalloy specimens simulating a blade root location in a gas turbine disc. Thus this type of equation appears often to be useful for constant amplitude fatigue crack growth analysis based on striation spacings, or at least worth trying. However, see subsection 4.2.

4.1 Example of striation-based modelling

Eijkhout (1994)^[11] developed an empirical model to describe the overall behaviour of MSD fatigue cracks in pressure cabin longitudinal lap splices. The model is based on the following observations:

- (1) MSD fatigue cracks tended to initiate at several sites close to the rivet holes, and grew in directions varying gradually from transverse to longitudinal, see the top diagram in figure 3.
- (2) The transverse (through-thickness) striation spacings (and hence fatigue crack growth rates) were virtually constant, see the upper graphic in figure 3.
- (3) Transverse and longitudinal striation spacings (and hence fatigue crack growth rates) were similar for crack dimensions less than twice the sheet thickness: compare the graphics in figure 3.

Figure 4 is a schematic of the model. There are three main assumptions, the first two of which are derived from the foregoing observations. The assumptions are:

- Constant fatigue crack growth rate in the transverse direction, in general equal to the *initial* crack growth rate in the longitudinal direction, i.e. $dc/dN = Ae^{Bai}$.
- Crack depth $c = 0$ at a_i , the "initiation length".
- Quarter-circular crack fronts in the transition from transverse to longitudinal crack growth.

These assumptions are convenient but not essential to the model's use. For example, the model can be used for non-constant dc/dN , and for crack initiation at rivet hole corners, i.e. $a_i = 0$ in figure 4. Also, the model can be used for both non-countersunk and countersunk lap splice sheets (Eijkhout 1994)^[11].

Figure 5 illustrates the use of the model. One can see that besides providing estimates of the fatigue crack "initiation" and growth lives, the model also enables estimates of the lives at which cracks become through-thickness. This latter information is potentially useful for in-service NDI, notably for visual inspection of the lap splice outer sheet.

4.2 Example of striation-based analysis unsuited to modelling

There are cases where striation-based crack growth equations and modelling cannot be used. Recourse must then be made to *the basic approach*. This is illustrated with the aid of figure 6.

The macrofractograph in figure 6 shows a fatigue crack in a vertical stabilizer rib from a full-scale test. The crack initiated and grew from a bolt hole during 180,000 simulated flights of *effectively* constant amplitude loading, whereby one cycle equalled one flight.

Fatigue striation spacings (one striation = one simulated flight) were measured along a near-surface crack path and are plotted in the upper diagram in figure 6. As such, these data look unpromising. However, the number of flights during crack growth can be estimated by taking the average striation spacing between each measurement interval, dividing this striation spacing into the interval, and adding up the numbers for each interval. The result is shown in the lower diagram.

The lower diagram in figure 6 gives an estimate of the overall crack growth behaviour. Despite the unpromising-looking striation measurements, the overall crack growth curve shows clearly that the crack slowed down when it started to grow into the web of the rib. Also, and more importantly, back-extrapolation indicates that a regular process of fatigue crack growth began from the bolt hole only after about 105,000 simulated flights. Thus the crack growth life was about 75,000 flights.

5 Constant amplitude plus markers fractography

This category concerns constant amplitude fatigue tests with marker loads at specified intervals. The marker loads are generally chosen to create fractographically detectable meso- to microscopic features along the fatigue crack fronts, resulting in *marker bands*, while having a minimal influence on the constant amplitude fatigue crack growth process. This is not an easy task, although two examples will be given in subsections **5.1** and **5.2**.

Detailed fractography aims to detect the marker bands, as well as consider some or all of the observational aspects listed in table 3. A general procedure for detecting marker bands is given in figure 7 (see also figure 9 later on). This procedure has been verified for high temperature fatigue crack growth in a nickel-base superalloy (Wanhill *et al.* 1996)^[12] but is also applicable to other materials, e.g. aluminium alloys tested at ambient temperatures.

Marker bands may be used *alone* to analyse fatigue crack growth, albeit somewhat crudely, see subsection **5.1**. On the other hand, marker bands can be combined with striation spacing measurements, see subsection **5.2**. This latter method is preferable, provided that resolvable fatigue striations constitute much of the fatigue fracture topography.

5.1 Marker band analysis

Measurement of fatigue marker band positions gives basic data on crack lengths and depths *versus* numbers of cycles, and these data can be further analysed to obtain crack growth rates.

Figure 8 gives an example of the procedure for MSD fatigue cracks initiating near rivet holes in a pressure cabin longitudinal lap splice. The marker bands were obtained by applying a coded block of alternating full and reduced pressure cycles between blocks of 10,000 full pressure cycles (the basic constant amplitude loading). A description of the procedure follows:

- Figure 8a is a schematic of tracing marker bands back from the final crack front, which was at 60,000 cycles. Note that the first two marker bands are hypothesised to be undetectable.
- Figure 8b is a plot of faying surface crack lengths *versus* numbers of cycles obtained from many measurements according to the method in figure 8a. The measurements can be back-extrapolated to zero crack size to obtain individual, average, or lower and upper bound estimates of fatigue crack "initiation" lives. For example, back-extrapolation of the data in figure 8b gave the following lower and upper bounds: bay 3, $N_i = 10,000 - 15,000$ cycles; bay 4, $N_i = 5000 - 10,000$ cycles (Piascik and Willard 1997)^[13]. And, of course, N_i estimates enable direct estimates of fatigue crack growth lives, since the total test life will be known.
- Figure 8c illustrates the somewhat crude method of using marker bands to determine fatigue crack growth rates *versus* crack size. Crack sizes are measured from the initiation site via the

approximate centres of the marker bands. Then the average crack growth rates and crack lengths are calculated as shown in figure 8c. Note that estimating the crack growth rate before the first observed marker band (marker #1) requires values of N_i and hence N to be estimated from plots like figure 8b, whereby $N - N_i \leq 10,000$ cycles.

- Finally, figure 8d gives an example of using marker bands to determine fatigue crack growth rates *versus* crack size, in this case the faying surface crack length. The data show a reasonable overall trend. In other words, the number of measurements compensates for the limited accuracy of the method. Note also that differing estimates of N_i have a secondary influence relative to the data scatter.

5.2 Marker band + striation analysis

Assuming that striations are observable on much of the fatigue fracture surface, figure 9 gives the complete procedure (an extension of the procedure in figure 7) for detecting marker bands, measuring fatigue striation spacings, and analysing the data to obtain estimates of fatigue crack "initiation" and growth lives. Note that part of this procedure, listed under *data processing*, is an iteration whereby striation spacings can be used to locate all marker bands, some of which may have been undetected in the first part of the procedure.

In fact, iterative checks comparing marker band locations and striation spacings can also be essential for discounting features initially thought to be marker bands. Figure 10 gives a notable example. This shows a high temperature fatigue fracture surface which had poorly visible marker bands, though the last one could be detected by a change in oxidation interference colours. On the other hand, fatigue striations were readily measurable and enabled checking not only actual marker bands (1, 3+4, 6, 9 and 14), but also discounting many apparent ones.¹

¹ A likely explanation for the apparent marker bands is the well-known tendency to see linear or arcuate features where none are actually present, e.g. the Martian "canals".

6 Flight simulation plus markers fractography

This category concerns flight simulation loading fatigue tests with *intentional* marker features occurring at specified and recurring intervals such that they produce recognisable "striation" patterns on fatigue fracture surfaces. The marker features can be severe flights, usually containing peak loads, or individual large load excursions, depending on the spectrum.

It is important to note that a flight simulation load sequence containing severe flights or individual large load excursions does not necessarily provide good fracture surface "readability". For example, the well-known gust and manoeuvre spectra MiniTWIST and FALSTAFF do not provide fracture surface "readability" without modification (Ekvall *et al.* 1984; Van der Linden 1984)^[14,15]. This is an emphatic caution for those concerned with the development of load sequences for flight simulation fatigue tests.

How to make a flight simulation load sequence "readable" is discussed by Ekvall *et al.*, Van der Linden and others in several papers presented at the 58th Meeting of the AGARD Structures and Materials Panel in 1984 (AGARD 1984)^[16].

Given that a flight simulation load sequence *does* provide good fracture surface "readability", two more important points are made here:

- (1) "Striation" patterns can be observed down to crack sizes well below 1mm.
- (2) One obtains crack length, a , *versus* N directly: integration of periodic measurements (true striations) is not required.

Figures 11 – 13 illustrate the macroscopic to microscopic fractographic analysis of fatigue cracking under flight simulation loading that was developed to provide excellent fracture surface "readability" without unduly compromising the spectrum characteristics. The fatigue 'striation' pattern in figure 12 is due to the four severest flights in each block of 5000 simulated flights: the position of the severest flight, type A, is clearly recognisable. Figure 13 shows that this pattern could be traced back to a crack size of only 20 μ m.

Note that back-extrapolation of the a *versus* N curve in figure 13b is uncertain. There was no initial defect with a size of 15 μ m. Instead it appeared that fatigue initiated in a single grain, possibly resulting in a crack only after many thousands of simulated flights. Be that as it may, a crack detectable by Non-Destructive Inspection (NDI) would have been much longer and well along the crack growth curve shown in figure 13a.

In other words, even though there may be uncertainty as to the fatigue "initiation" life, data like those in figure 13 can be most useful for determining in-service NDI schedules.

7 Spectrum fatigue analysis

This category concerns flight simulation loading fatigue tests whose load sequences have not been modified to ensure fracture surface "readability" and, most importantly, service fatigue cracking.

In both cases it is often uncertain whether the load history will have resulted in fatigue striations or "striation" patterns that can be fractographically analysed. Two examples where this was possible were mentioned at the beginning of section 4, namely high-cycle fatigue of a helicopter rotor blade (Wanhill *et al.* 1974)^[8], and MSD fatigue in pressure cabin longitudinal lap splices (Wanhill *et al.* 2001)^[7].

Two more examples are described in subsections 7.1 and 7.2. The first concerns fatigue cracks at fastener holes in GLARE (GLASS REinforced aluminium laminate) panels and aluminium alloy window frames from the Airbus MegaLiner Barrel (MLB) test.

The second is an in-flight failure of an air supply manifold support rod from a military jet engine. This failure was particularly interesting owing to the diagnostic assistance of oxidation interference colours on the fatigue fracture surfaces.

7.1 Airbus MLB window area fractography

The MLB pressure cabin test was run to 45,402 simulated flights using a complicated fatigue load spectrum. Figure 14 shows the window area shortly after removal from the MLB. The basic structure is a GLARE skin fastened with Hi-Loks to aluminium alloy window frames. The GLARE skin was seven 2024-T3 aluminium alloy layers 0.3mm or 0.4mm thick interleaved with six glass fibre layers.

After teardown and NDI (Platenkamp *et al.* 2005)^[18], the largest fastener hole crack in either window frame was forcibly opened, as illustrated in figure 2, and fractographically analysed to check for spectrum "readability".

Figure 15 gives an example of detecting the simulated flights, notably the severest flight types A, B and C. Despite the complexity of the spectrum, the "readability" was excellent, enabling crack growth to be traced back from 1.68mm at the end of the test to less than 0.2mm. This was necessary to obtain:

- Fatigue crack growth curves
 - a *versus* N
 - da/dN *versus* a*
- An estimate of fatigue "initiation" life.

where a* is the mean of the crack growth interval used to calculate da/dN.

Figures 16a and 16b present the crack growth curves. Both figures show the effects of severe flights, pointed out explicitly in figure 16b. Most of these effects appear to be transient. However, beginning at a crack length of 0.6mm there was a significant and persistent retardation of fatigue crack growth. This persistent retardation could be due to termination of the “short crack effect”. This effect is well known, and is generally attributed to a lack of fatigue crack closure in cracks smaller than about 0.5mm. Thus once the crack in the window frame grew beyond about 0.5mm, closure-induced retardation effects of peak loads in severe simulated flights would have become possible.

Back-extrapolation of the *a versus N* curve in figure 16a suggests that the fatigue “initiation” life was zero, and that there was an initial crack size of about 0.06mm. In fact, the crack initiated from a fretting scar (Wanhill *et al.* 2006)^[19]. This explains the effectively zero fatigue “initiation” life and also the indication of an initial crack size.

The largest fastener hole crack in the GLARE skin was also fractographically analysed. To enable this, the cracked hole was forcibly opened (Wanhill *et al.* 2006)^[19] and one fracture surface was exposed to a low-temperature oxygen plasma for 30 – 45 minutes. This degraded the interlayer adhesive, allowing easy separation of the aluminium and glass fibre layers. However, the sample temperatures remained below 60 – 80°C, which meant that the aluminium fatigue fracture surfaces were undamaged. Then the aluminium layer with the largest fatigue crack could be examined under optimum conditions in a FEG-SEM.

The largest “readable” aluminium layer crack was 0.91mm long. Crack growth could be traced back only to 0.45mm, below which the crack front markers were impossible to resolve.

Figures 17a and 17b present the crack growth curves. The data are limited, but sufficient to show that the “plateau” crack growth rates were about 50% of those in the aluminium window frame.

Back-extrapolation of the *a versus N* curve in figure 17a is unfeasible, owing to the limited data. Hence an estimate of the fatigue “initiation” life is not possible.

7.2 Air supply manifold support rod failure

Bending fatigue failure occurred in a support rod linking the bleed air supply manifold to the diffuser case in a military jet engine. Figure 18 shows the location of the support rod with respect to the diffuser case, and table 4 gives the engine operating history.

Table 4 Incident engine operating history

Service history (M= maintenance)	Intervals	
	Hours	Flights
0 → M(1)	410.9	257
M(1) → M(2)	761.5	326
M(2) → failure	143.5	57

The rod was wrought Inconel 718, a nickel-base superalloy, operating in air at about 550°C. Figure 19 shows a macrophotograph and schematic of the fracture surface of the broken rod. There were two fatigue areas. The older fatigue area was centred on the 2 o'clock position and showed both first and second order interference colours due to oxidation. The more recent main fatigue crack was centred on the 6 o'clock position and showed first order interference colours only, with narrow bands of contrasting colours on the light blue to yellow part of the fracture surface.

The main fatigue fracture surface consisted of Stage I and Stage II fatigue (Wanhill 2004)^[10], see figure 19b. The Stage II fatigue surface was SEM-mapped completely at 200×, with details up to 1000×. This surface was almost completely covered by striations, with periodic large striations that resulted in “beach” marks.

Striation spacing measurements gave an estimate of 14,500 cycles for the entire Stage II region, i.e. this was Low-Cycle Fatigue (LCF). However, the “beach” marks were potentially of more interest because they represented peak load excursions during engine operation, and might enable estimating the number of flights during Stage II fatigue crack growth.

The “beach” marks were counted by two independent fractographers. Figure 20 shows the results related to the main crack depth and the broad divisions of interference colours. If the “beach” marks were to correspond to start-stop cycles of the engine, then figure 20 would indicate a Stage II fatigue crack growth life of about 250 flights.

To check this, the service maintenance history was compared with the *total* fracture surface appearance of the broken rod and the results of 550°C furnace oxidation tests. These tests were

done on Inconel 718 fatigue fracture surfaces obtained at room temperature and having a similar topography to the main Stage II fracture surface of the broken rod.

The oxidation tests indicated that the main Stage II fatigue fracture surface of the broken rod could not have been older than about 370 hours, and was probably much less (Wanhill 2004)^[10]. This information, together with the maintenance history in table 4 and the total fracture surface appearance, led to the following interpretation, see figure 21:

The older, secondary fatigue crack, area (1), occurred during the period up to the first maintenance. Then the rod was reinstalled with a chance axial rotation that inhibited further growth of this crack.

- The main fatigue crack initiated between the first and second maintenances, and the second maintenance hardly altered the rod's orientation. However unlikely this might seem, the alternative would be that the entire main fatigue crack initiated and grew during the 143.5 operating hours from the second maintenance to failure. This is incompatible with the interference colour evidence: a fully or largely silvered Stage I area must have required several hundred operating hours. In fact, it seems likely that most – if not all – of the crack growth in area (2) occurred during the period between the first and second maintenance.
- This leaves the period from the second maintenance to failure, 143.5 operating hours, as the maximum time to form the fatigue crack growth area (3).

The foregoing rationale is compatible with the interference colours on the fatigue fracture surface. Furthermore, there were about 55 – 60 of the narrow bands of contrasting colours on area (3). This number agrees well with the number of flights, 57, from the second maintenance to failure, and is likely to be no coincidence. In other words, these narrow bands probably represent oxidation effects due to flight-by-flight heating and cooling.

Summarizing, the comparison of maintenance history, the time dependence of the oxidation interference colours, and the narrow bands of contrasting colours indicated that Stage II fatigue crack growth took place between the second maintenance and failure. Thus the number of “beach” marks, estimated to be about 250, had to correspond to a maximum of 57 flights, and therefore represent peak load excursions occurring more than once per flight. This is reasonable and normal for military jet engines.



8 Concluding remarks

The guidelines and procedures described and illustrated in this paper represent mainly, though not entirely, the accumulated knowledge from more than 30 years of fractographic analysis of fatigue fracture surfaces at the NLR.

These guidelines and procedures may be of assistance to others involved in fractographic investigations of fatigue failures in aircraft materials and components. However, there is no guarantee that any given fatigue fracture surface can be analysed in one of the ways described. In this respect it is recommended to develop and use fractographically “readable” fatigue load sequences for tests on full-scale structures and components.

References

1. S.P. Lynch, Progression Markings, Striations, and Crack Arrest Markings on Fracture Surfaces, Preprint of paper for the 2006 TMS Annual Meeting, March 2006, San Antonio, TX, USA.
2. I. Nedbal, J. Siegl, J.Kunz, Fractographic Study of Fatigue Crack Kinetics in Bodies and Structures, *Advances in Fracture Research (Fracture 84)*, *Proceedings of the 6th International Conference on Fracture (ICF6)*, (Editors S.R. Valluri, D.M.R. Taplin, P. Rama Rao, J.F. Knott and R. Dubey), Vol. III, Pergamon Press, Oxford, UK, 1984, pp. 2033- 2040.
3. I. Nedbal, J. Siegl, J. Kunz, Relation Between Striation Spacing and Fatigue Crack Growth Rate in Al-Alloy Sheets, *Advances in Fracture Research, Proceedings of the 7th International Conference on Fracture (ICF7)*, (Editors K. Salama, K. Ravi-Chandar, D.M.R. Taplin and P.Rama Rao), Vol. 5, Pergamon Press, Oxford, UK, 1989, pp. 3483-3491.
4. W.J. Plumbridge and D.A. Ryder, *Metals and Materials*, 1969, Vol. 3, pp. 321-344 (pp.119- 142 as Metallurgical Review 136).
5. H. Mughrabi, Microscopic Mechanisms of Metal Fatigue, *Strength of Metals and Alloys, Proceedings of the 5th International Conference*, (Editors P. Haasen , V. Gerold and G. Kostorz), Vol.3, Pergamon Press, Oxford, UK, 1980, pp. 1615-1638.
6. M.A. Jameel, P. Peralta and C. Laird, 2003, *Materials Science and Engineering A*, 2003, Vol. A342, pp. 279-286.
7. R.J.H. Wanhill, T. Hattenberg and W. van der Hoeven, A Practical Investigation of Aircraft Pressure Cabin MSD Fatigue and Corrosion, NLR Contract Report NLR-CR-2001-256, June 2001, National Aerospace Laboratory NLR, Amsterdam, the Netherlands.
8. R.J.H. Wanhill, E.A.B. de Graaf and W.J. van der Vet, Investigation into the Cause of an S- 61N Helicopter Accident. Part I: Fractographic Analysis and Blade Material Tests, NLR Technical Report NLR TR 74103 C, July 1974, National Aerospace Laboratory NLR, Amsterdam, the Netherlands.
9. T. Hattenberg and H. Vlieger, Fractographic Investigation of Cracks in Finger Strip (LHS) and Rib 5.0 (RHS) of Fin Found During the 2nd Phase of Fokker 100 TA-22B Testing, NLR Contract Report NLR CR 93265 C, June 1993, National Aerospace Laboratory NLR, Amsterdam, the Netherlands.
10. R.J.H. Wanhill, 2004 , *Journal of Failure Analysis and Prevention*, 2004, Vol.4 (Issue 1), pp. 53-61.

11. M.T. Eijkhout, Fractographic Analysis of Longitudinal Fuselage Lapjoint at Stringer 42 of Fokker 100 Full Scale Test Article TA15 after 126250 Simulated Flights, Fokker Report RT2160, November 1994, Fokker Aircraft Ltd., Amsterdam, the Netherlands.
12. R.J.H. Wanhill, T. Hattenberg and H.J. ten Hoeve, Fractographic Examination of Three EGT Rim Specimens, NLR Contract Report NLR CR 96451 C, July 1996, National Aerospace Laboratory NLR, Amsterdam, the Netherlands.
13. R. S. Piascik and S. A. Willard, The Characteristics of Fatigue Damage in the Fuselage Riveted Lap Splice Joint, NASA Technical Publication NASA/TP-97-206257, November 1997, National Aeronautics and Space Administration Langley Research Center, Hampton, VA, USA.
14. J.C. Ekvall, L. Bakow and T.R. Brussat, Periodic Loading Sequences for the Systematic Marking of Fatigue Crack Fracture Surfaces, *Fatigue Crack Topography*, AGARD Conference Proceedings No. 376, Advisory Group for Aerospace Research and Development, Neuilly sur Seine, France, November 1984, pp. 10-1–10-9.
15. H.H. van der Linden, Modifications of Flight- by-Flight Load Sequences to Provide for Good Fracture Surface Readability, *Fatigue Crack Topography*, AGARD Conference Proceedings No. 376, Advisory Group for Aerospace Research and Development, Neuilly sur Seine, France, November 1984, pp. 11-1–11-22.
16. AGARD Conference Proceedings No. 376, *Fatigue Crack Topography*, Advisory Group for Aerospace Research and Development, Neuilly sur Seine, France, November 1984.
17. T. Hattenberg, Fractographic Investigation of Cracks Found in Vertical Stabilizer Main Hinge Fitting During the 2nd Phase of Fokker 100 TA- 22B Testing, NLR Contract Report NLR CR 94213 C, May 1994, National Aerospace Laboratory NLR, Amsterdam, the Netherlands.
18. D.J. Platenkamp, A.F. Bosch, R.J.H. Wanhill and T. Hattenberg, MegaLiner Barrel Teardown Programme. Part 1: NDI Test Results for the F4 Window Panel, NLR Contract Report NLR-CR- 2005-665, December 2005, National Aerospace Laboratory NLR, Amsterdam, the Netherlands.
19. R.J.H. Wanhill, T. Hattenberg, D.J. Platenkamp and A.F. Bosch, MegaLiner Barrel Teardown Programme. Part 2: Fractographic Examination and Analysis of Fatigue Cracks for the F4 Window Panel, NLR Contract Report NLR-CR- 2005-666, April 2006, National Aerospace Laboratory NLR, Amsterdam, the Netherlands.

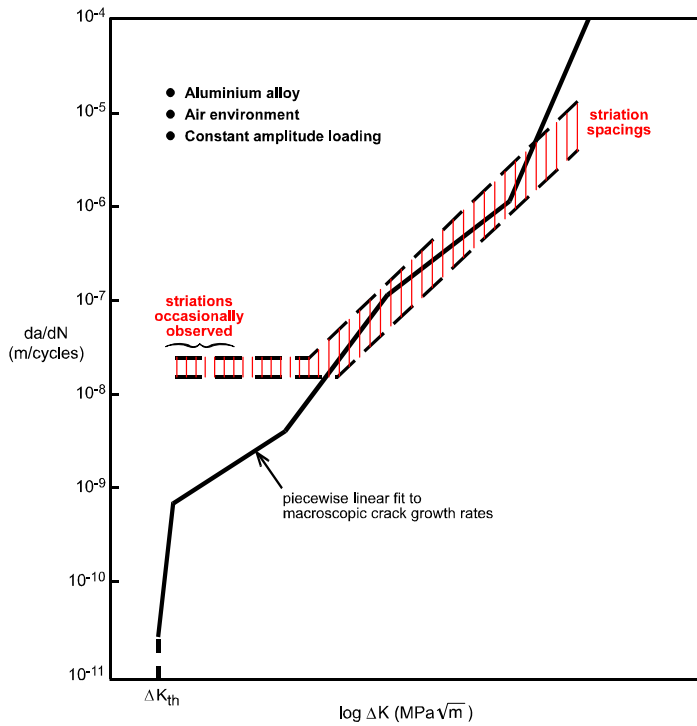


Figure 1 Schematic fatigue crack growth diagram assuming constant amplitude loading and a normal air environment

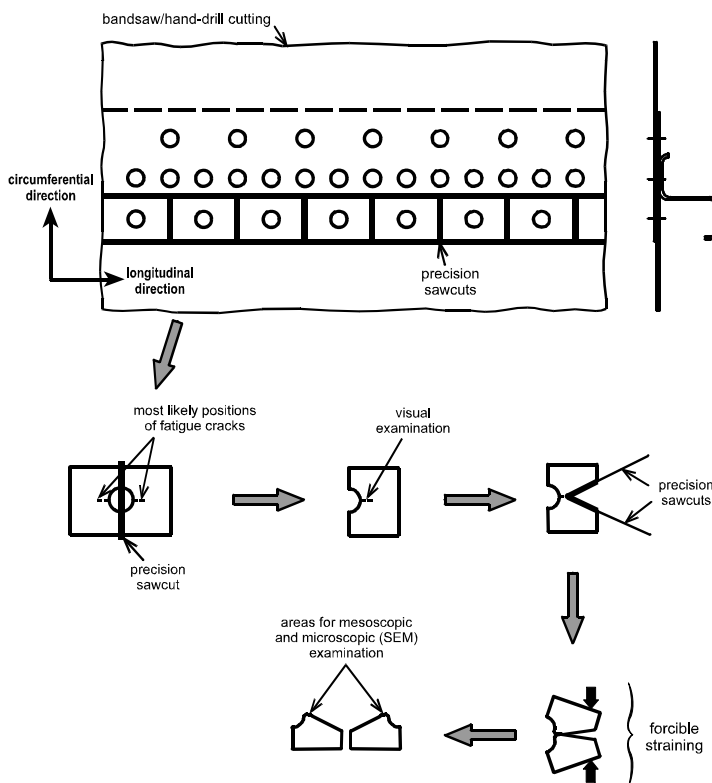


Figure 2 Illustration of opening up cracks: MSD fatigue in pressure cabin longitudinal lap splices (Wanhill et al. 2001)^[7]

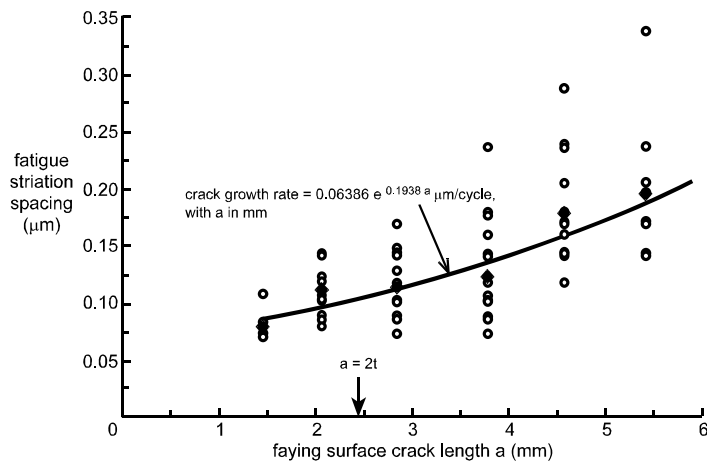
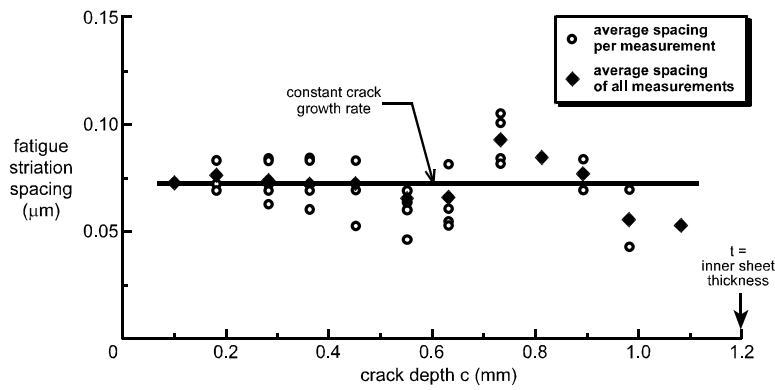
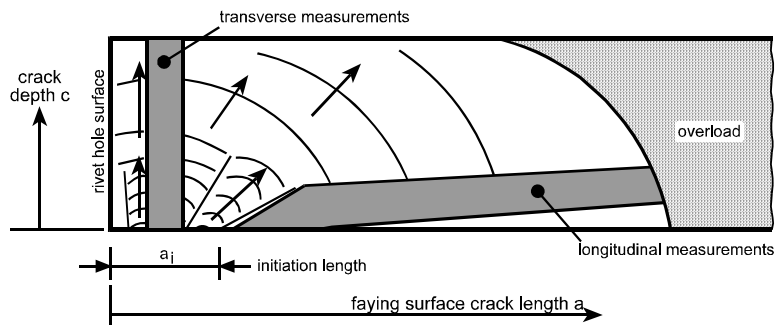
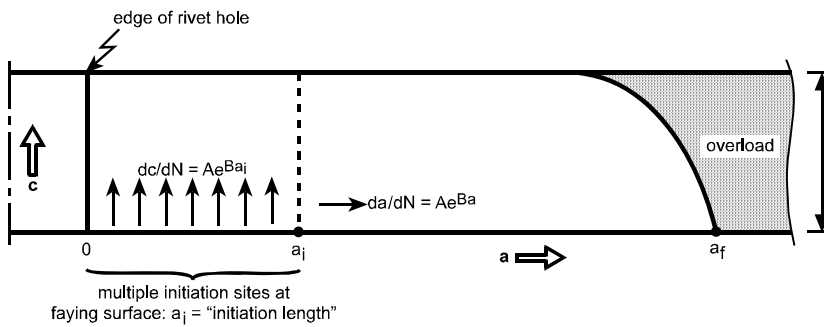


Figure 3 Example of striation measurements in selected directions: MSD crack from the faying surface of a pressure cabin longitudinal lap splice (Wanhill et al. 2001)^[7]. Note the multiple initiations constituting an initiation “length”

- From fractographic observations and striation spacings:



- a_i , a_f and N_f are known. Calculate N_i from:

$$N_f - N_i = \frac{1}{AB} (e^{-Ba_i} - e^{-Ba_f})$$

- Calculate intermediate values of a for given values of N :

$$a_{int} = -\frac{1}{B} \ln [e^{-Ba_i} - AB(N_{int} - N_i)]$$

- For each a_{int} calculate c_{int} from:

$$c_{int} = (N_{int} - N_i) AeBa_i$$

- Construct crack fronts as follows:

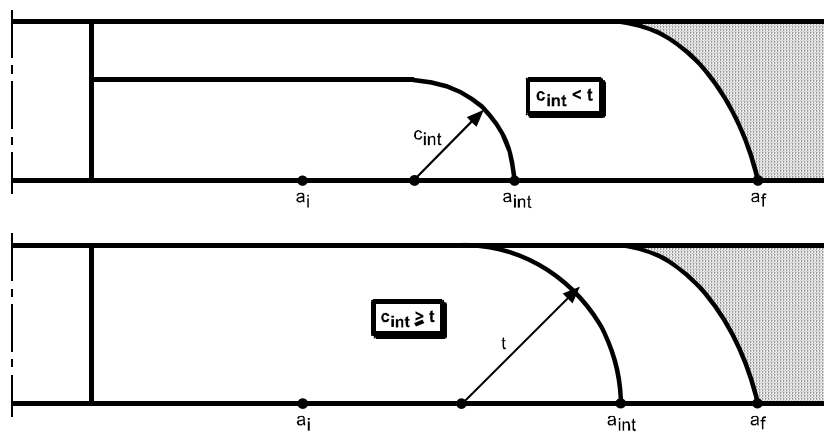


Figure 4 MSD model (Eijkhout 1994)^[11], shown for a non-countersunk sheet and multiple fatigue initiation sites

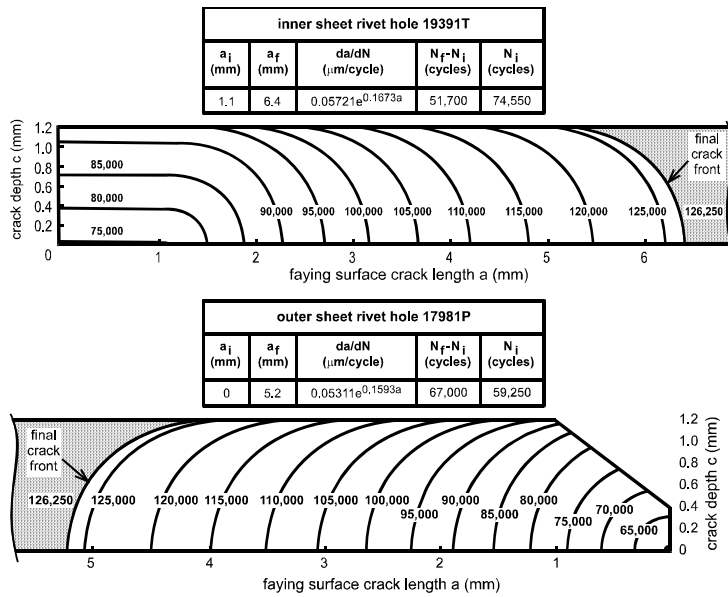


Figure 5 Examples of the use of Eijkhout's model to predict "iso-life" fatigue crack fronts for two MSD fatigue cracks

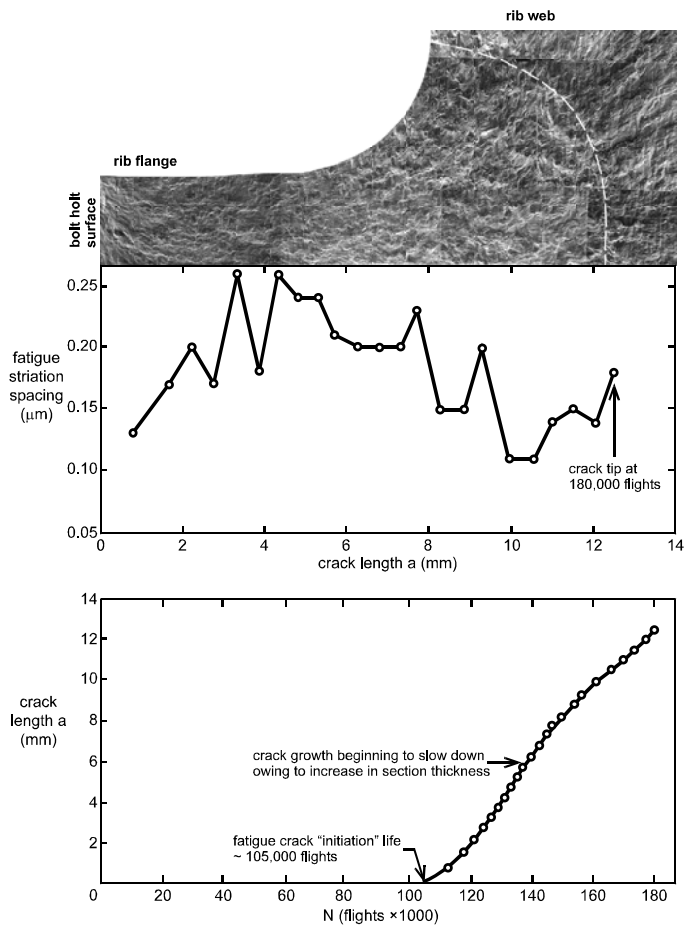


Figure 6 Striation-based analysis of crack growth from a bolt hole in a vertical stabilizer rib (Hattenberg and Vlieger 1993)^[9]

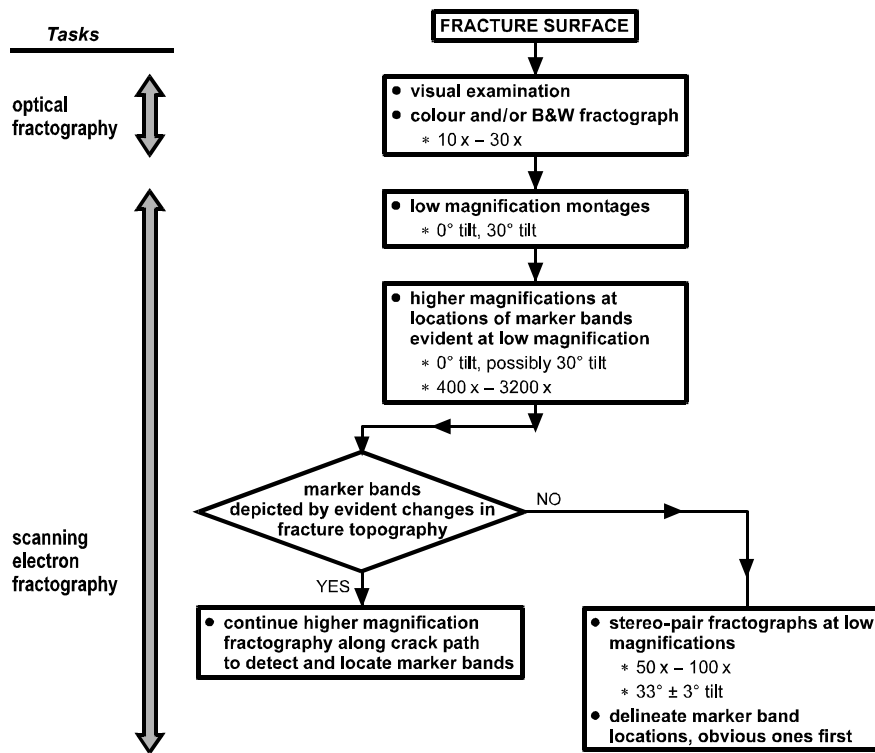
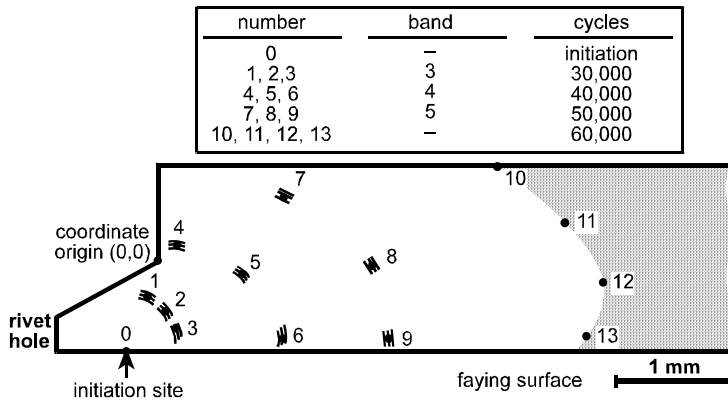
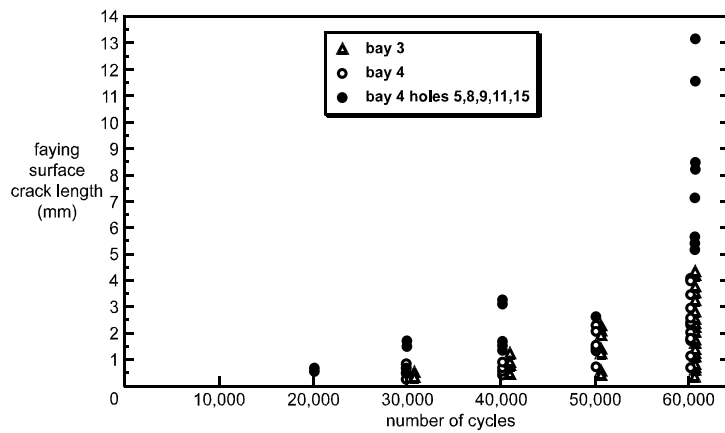


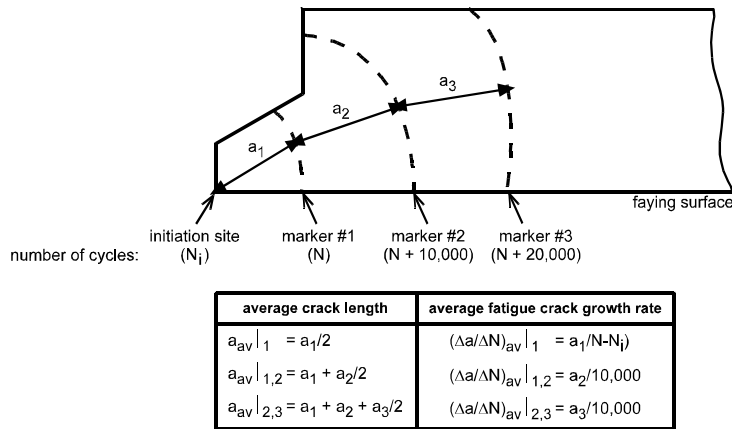
Figure 7 Detection of marker bands on fatigue fracture surfaces (Wanhill et al. 1996)^[12]



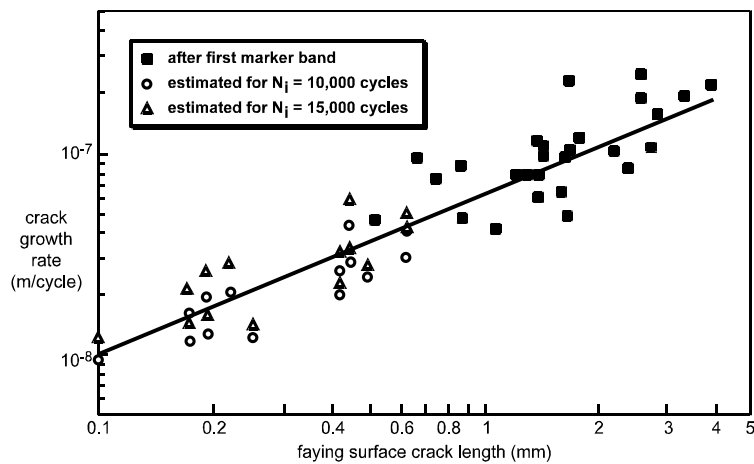
(a) Example schematic of MSD with marker bands



(b) MSD actual crack lengths *versus* cycles



(c) Schematic of method to determine crack growth rates *versus* crack length or depth from marker bands. Values of N_i and hence N have to be estimated from plots like figure 8b



(d) MSD crack growth rates *versus* crack length for two estimates of N_i

Figure 8 Marker band analysis for an outer sheet upper rivet row of a test article pressure cabin longitudinal lap splice (Piascik and Willard 1997)^[13]

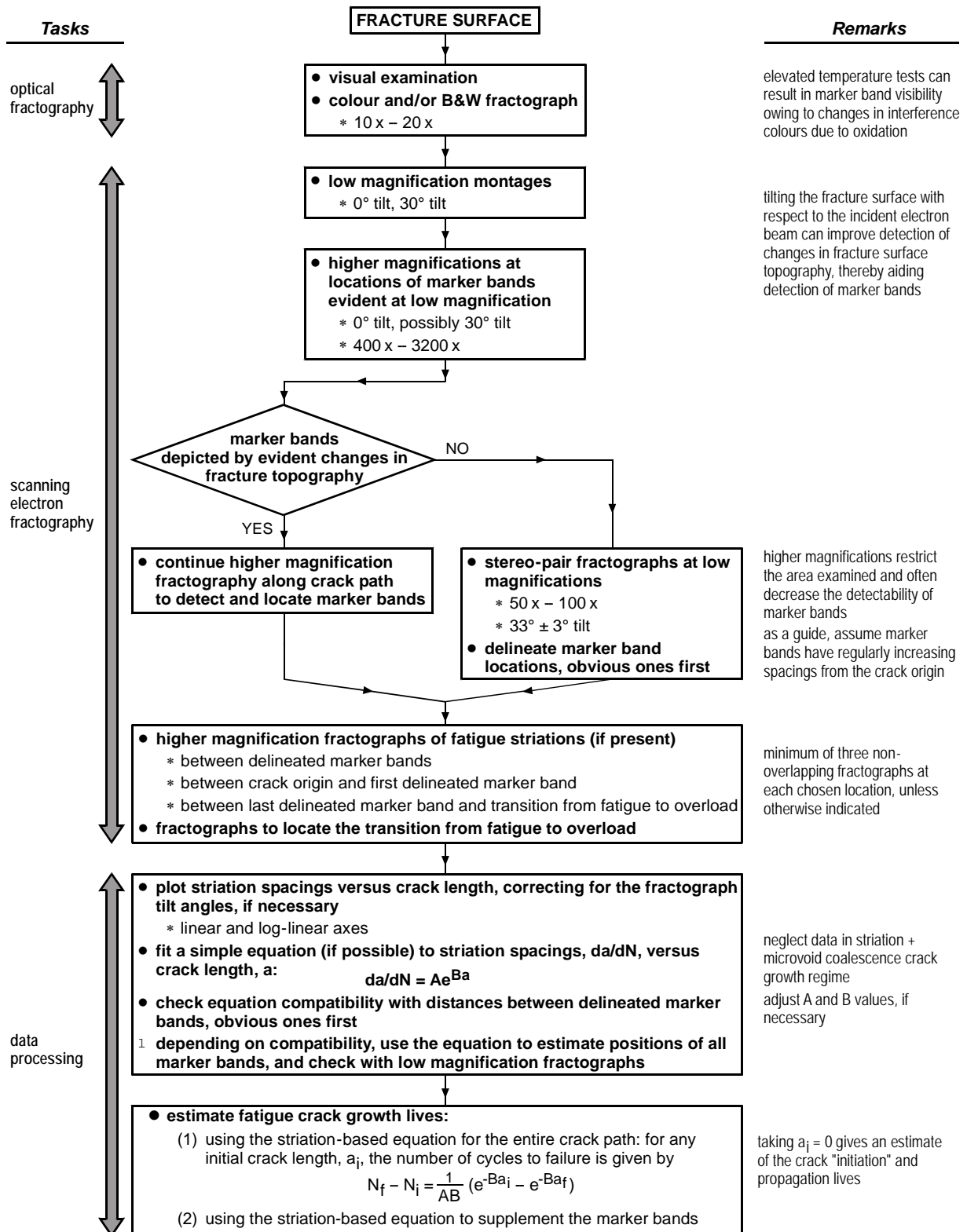


Figure 9 Fractography-based method of estimating fatigue crack "initiation" and growth lives and fatigue crack growth rates for specimens tested under constant amplitude loading interspersed with marker band loading, at ambient or elevated temperatures (Wanhill et al. 1996)^[12]. The method assumes that striations are observable on much of the fatigue fracture surface

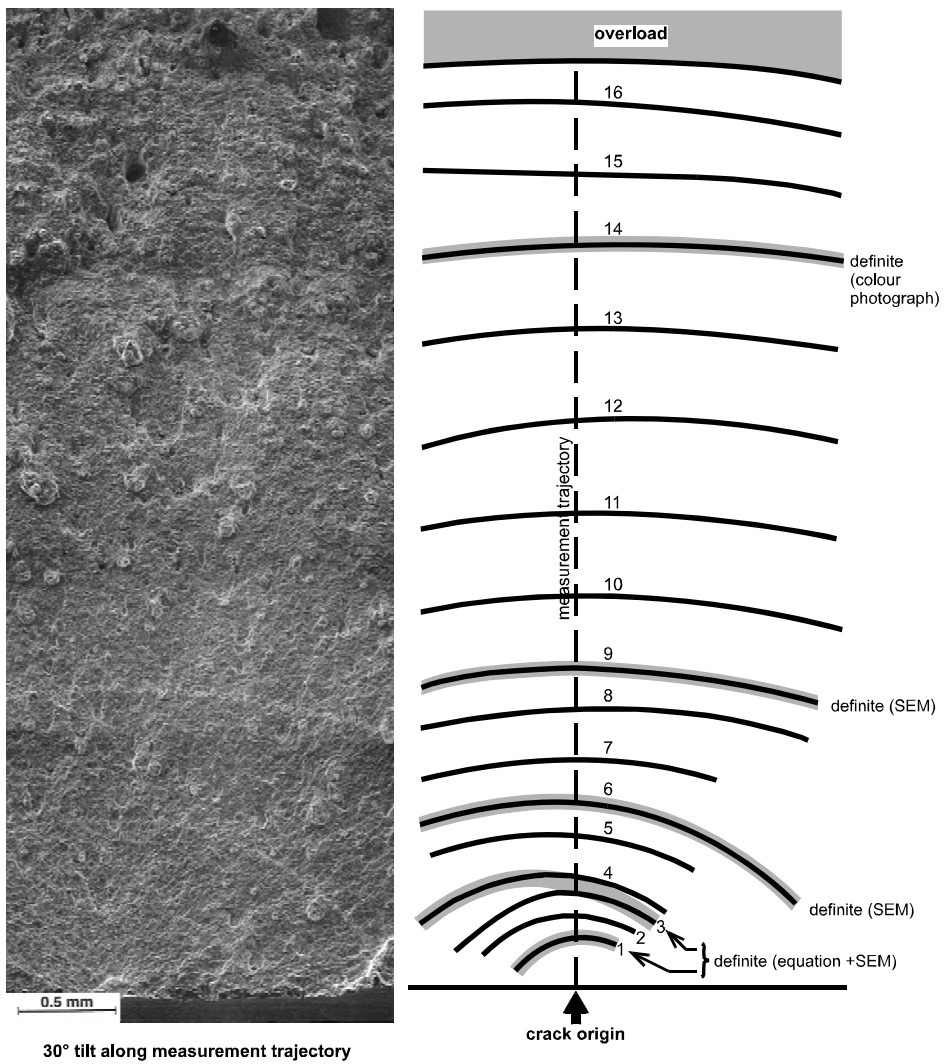


Figure 10 Low magnification SEM fractographic montage and marker band locations for a nickel-base superalloy (Inconel 718) specimen fatigue tested under constant amplitude + marker band loading at 600°C in air (Wanhill et al. 1996)^[12]

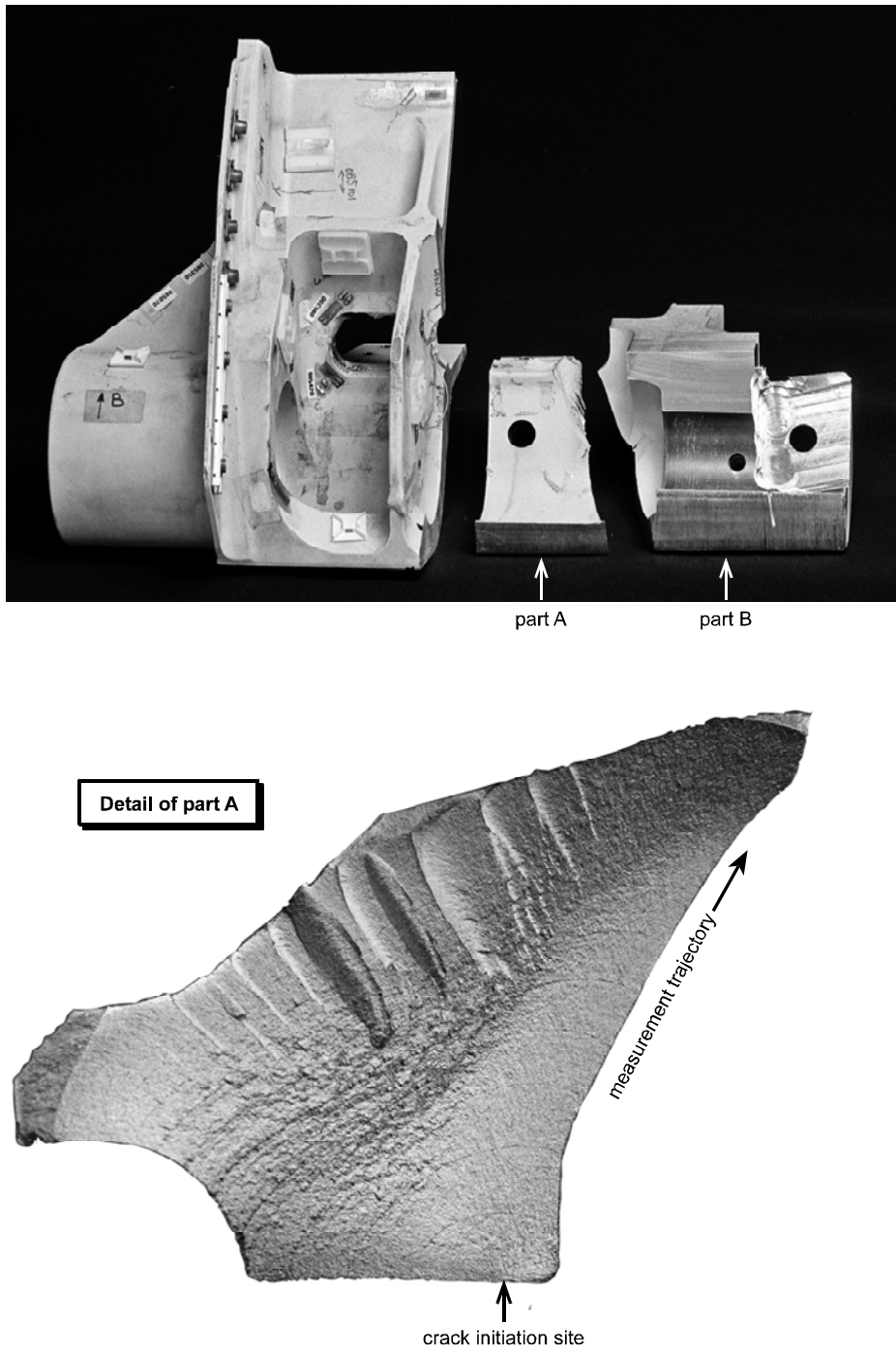


Figure 11 Overview and macroscopic fractograph of the fatigue fracture surface of a crack in a vertical stabilizer main hinge fitting (Hattenberg 1994)^[17]

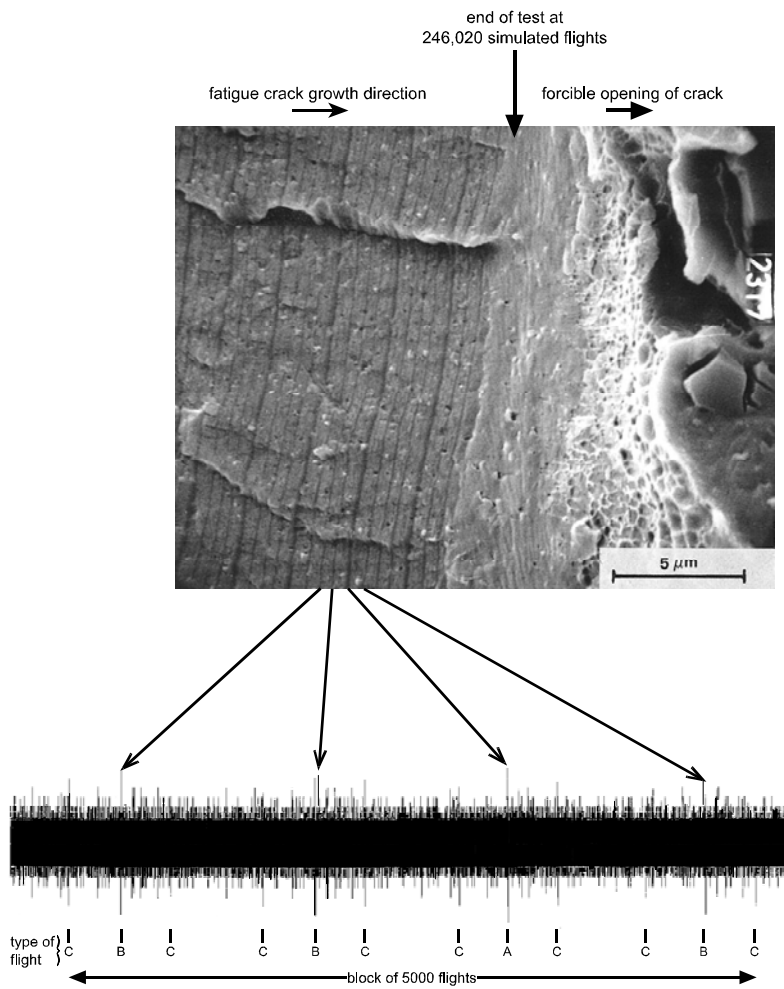


Figure 12 Illustration of the fatigue “striation” pattern owing to repeated blocks of 5000 simulated flights in the gust spectrum loading of a vertical stabilizer (Hattenberg 1994)^[17]

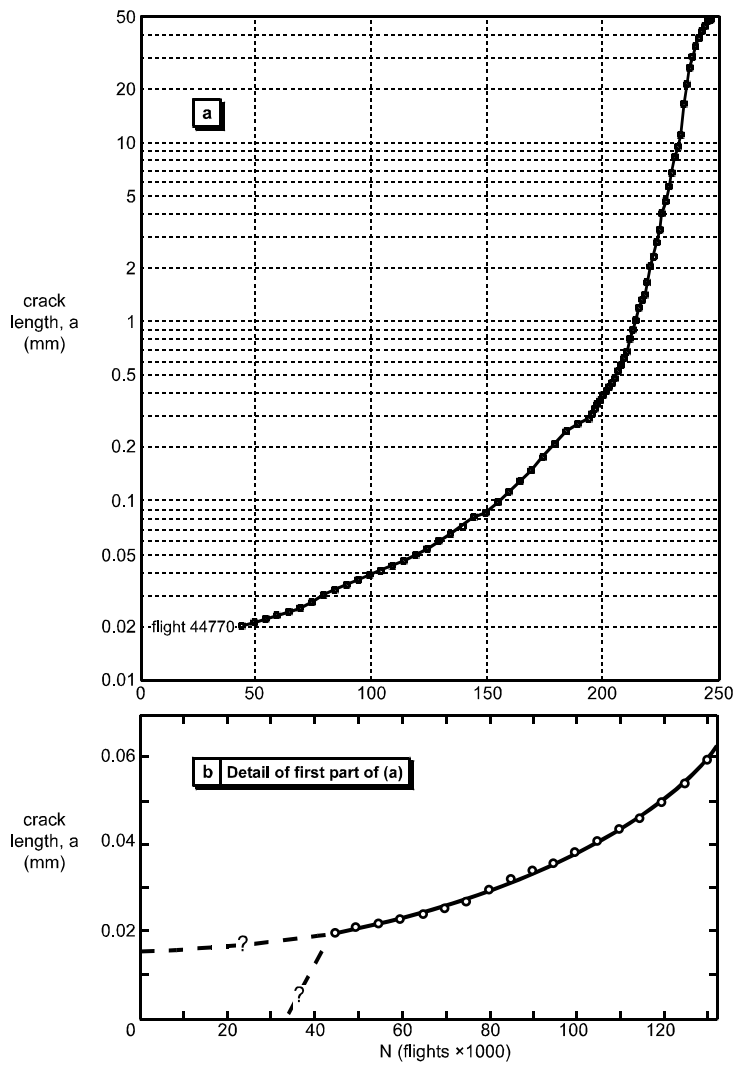


Figure 13 "Striation" pattern analysis of fatigue crack growth in a vertical stabilizer main hinge fitting (Hattenberg 1994)^[17]



Figure 14 GLARE window area cut from the MLB

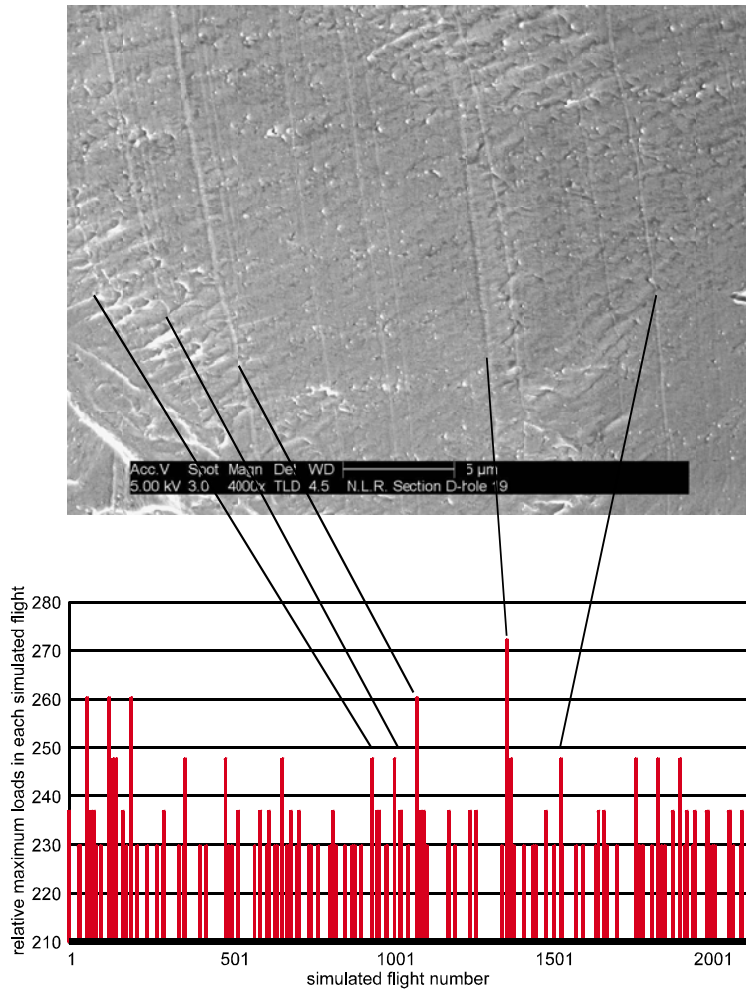
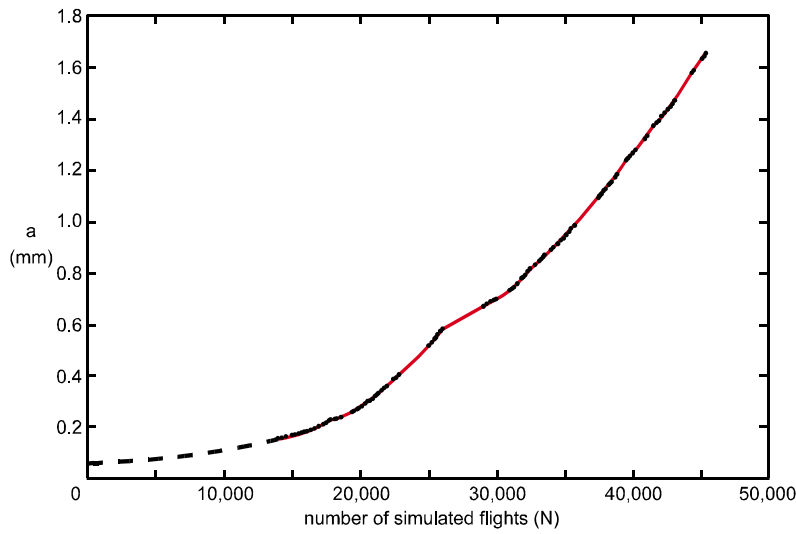
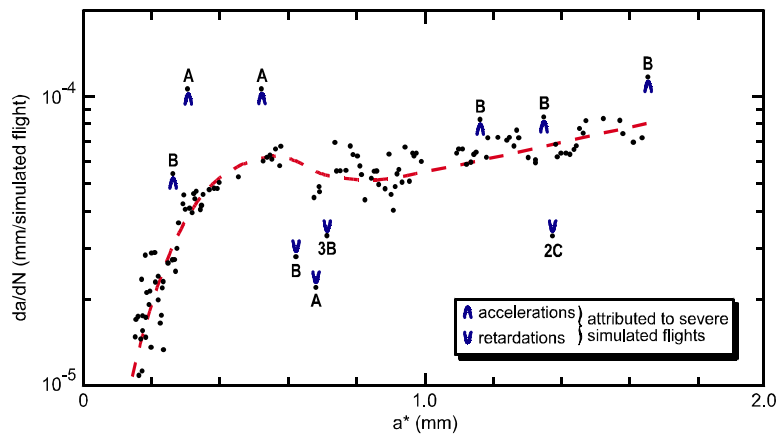


Figure 15 Example of fractographic identification of severe simulated flights in the MLB fatigue load spectrum, using the largest window frame crack

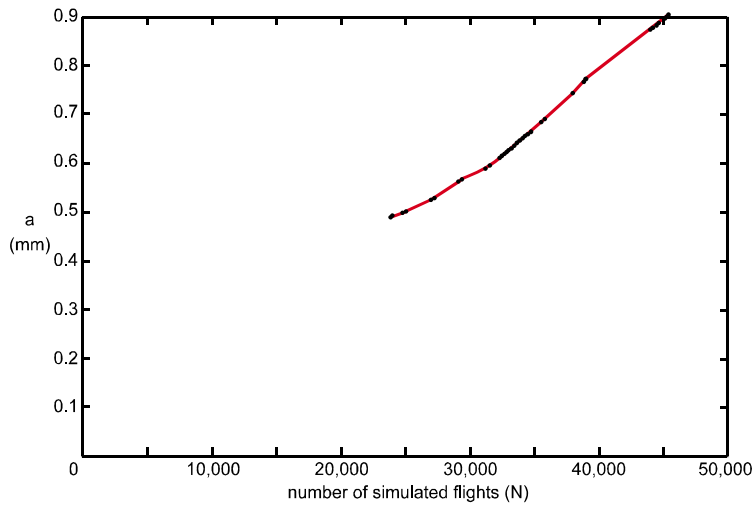


(a) Crack length *versus* number of simulated flights

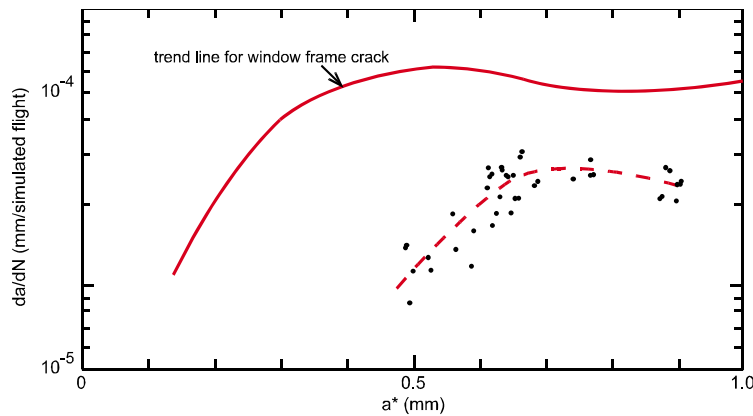


(b) Crack growth rates *versus* mean crack lengths

Figure 16 Crack growth curves for the largest fastener hole crack in either of the window frames. The material was die forged aluminium alloy 7175-T73



(a) Crack length *versus* number of simulated flights



(b) Crack growth rates *versus* mean crack lengths

Figure 17 Crack growth curves for the largest “readable” fastener hole crack in an aluminium layer of the GLARE skin. The material was 0.3mm 2024-T3 sheet

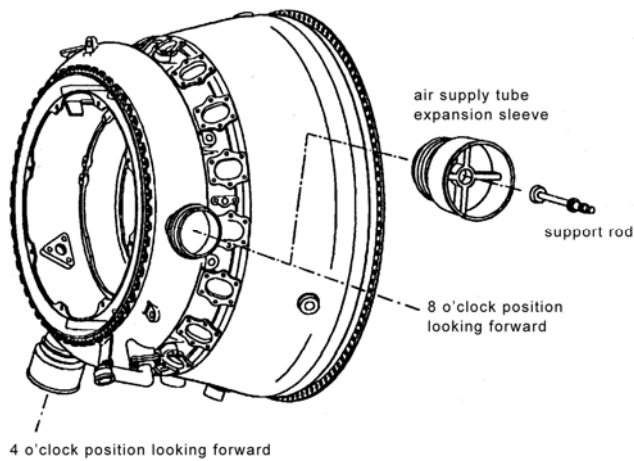


Figure 18 Diffuser case and one air supply tube expansion sleeve and a support rod (broken in the incident engine)

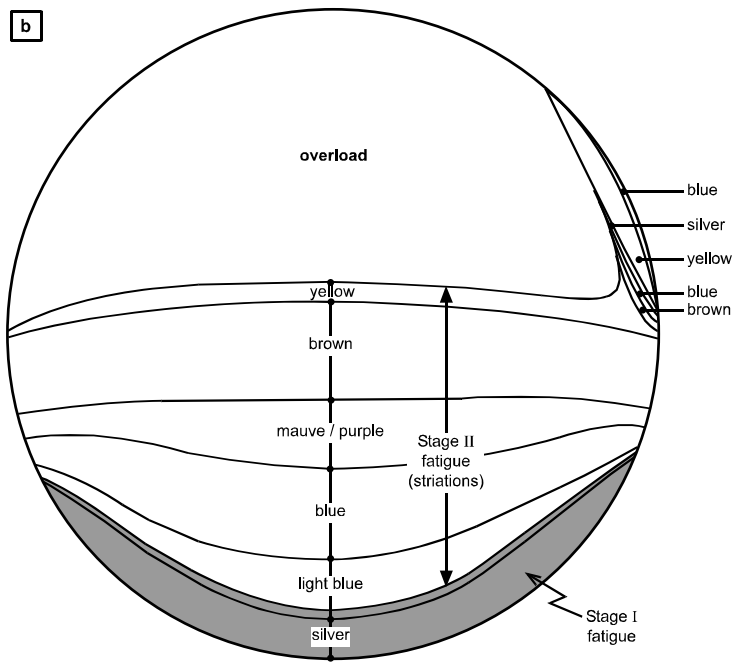
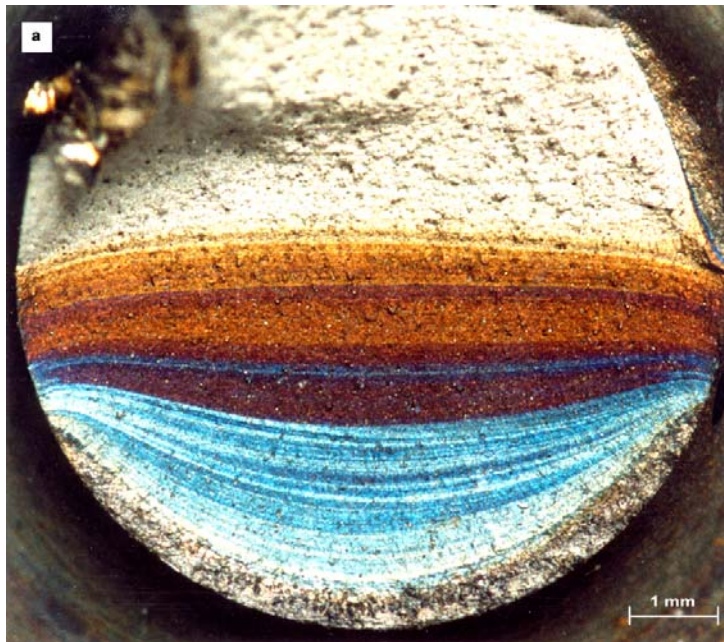


Figure 19 Macro photograph and schematic of the fracture surface of the broken rod

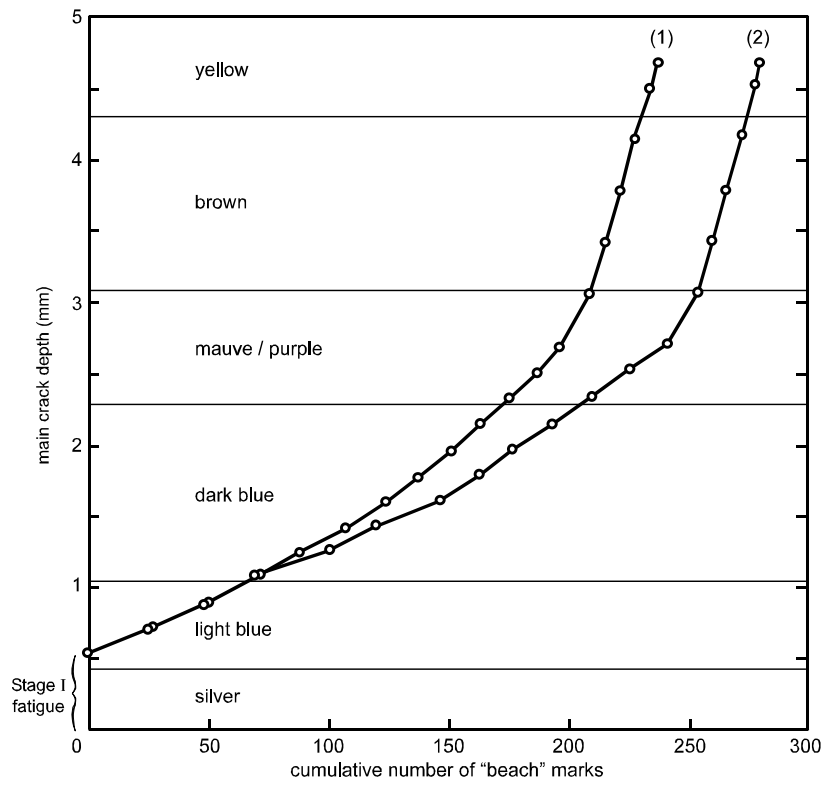
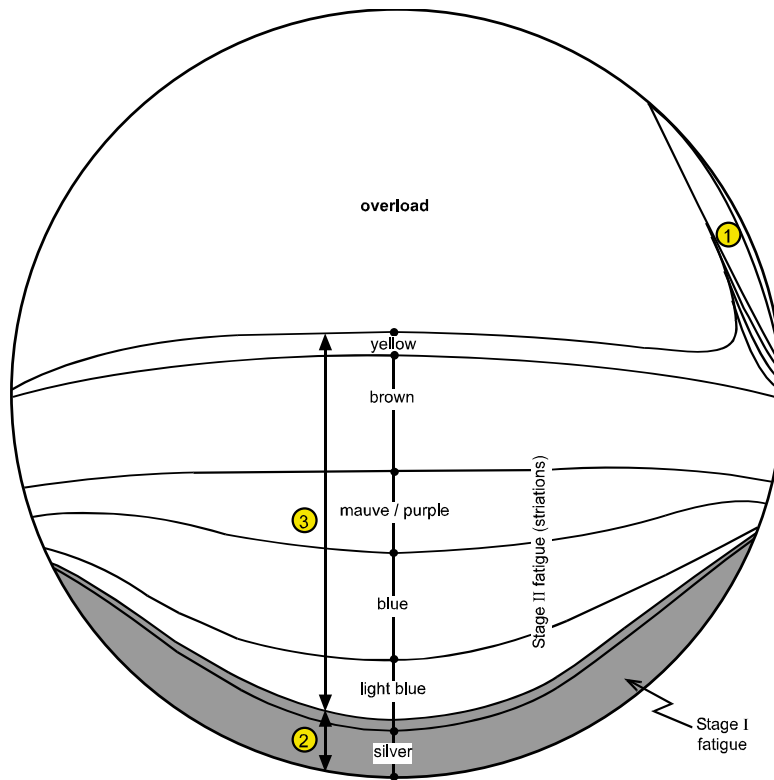


Figure 20 Cumulative number of "beach" marks for the Stage II fatigue region of the main fatigue fracture surface of the broken rod. (1) and (2) are independent measurements by two fractographers



Service history	Intervals		Fatigue fracture areas
	Operating hours	Flights	
0 → 1st maintenance rod rotation	410.9	257	①
1st → 2nd maintenance no rod rotation	761.5	326	②
2nd maintenance → failure	143.5	57	③

Figure 21 Interpretation of the relation between service history and fatigue fracture areas for the broken rod